Supporting Information

Surface-Engineered Asymmetric Hollow Fiber Membranes with Facilitated Transport Interfaces for CO_2 Capture

Jiayou Liao*,†[a,b] Shouwei Liu,† [a] Xinyue Meng ,†[a] Chengyun Gao,[c] Xianjie Meng, [a] Zhichao Zhai,[a] Shuangming Wang,[a] Yong Wang,[a,b] Xu Wu*,[a] and Jinping Li* [a,b]

a. Taiyuan University of Technology, Taiyuan 030024, Shanxi (PR China).
b. Shanxi Research Institute of Huairou Laboratory, 030032, (PR China).
c. Taiyuan University of Science and Technology, Taiyuan 030024, (PR China).
† These authors contributed equally to this work.

The results demonstrate that as the degree of bromination increases, both the number-average molecular weight (Mn) and weight-average molecular weight (Mw) of the polymers exhibit a downward trend, accompanied by a progressive broadening of the polydispersity index (PDI) from 2.22 to 4.6. This phenomenon is primarily driven by the highly reactive bromine radicals, which inevitably subject the polyimide backbone to random attacks, thereby inducing mild chain scission. This effect is particularly pronounced at high bromination levels (50%–100%), where the drastic increase in steric hindrance further elevates the probability of backbone degradation. Because Mn is inherently more sensitive to the low-molecular-weight fragments generated during this process, it declines at a faster rate than Mw, resulting in the observed broadening of the molecular weight distribution. Nevertheless, despite the unavoidable chain degradation associated with free-radical mechanisms, the Mw of the sample remains remarkably high at 209 kDa, even at 100% bromination. This robust retention of molecular weight ensures that the PI-Br polymer series maintains excellent mechanical stability for subsequent surface chemical cross-linking.

Table. S1 GPC Analysis of Bromination Process

Sample	Mn (Da)	Mw (Da)	Polydispersity Index (PDI)
Pristine PI (6FDA-DAM)	113,995	252,746	2.22
PI-Br-10%	108,814	249,029	2.29
PI-Br-30%	99,986	243,736	2.43
PI-Br-50%	87,577	235,444	2.69
PI-Br-70%	69,780	224,965	3.22
PI-Br-100%	45,454	209,612	4.6

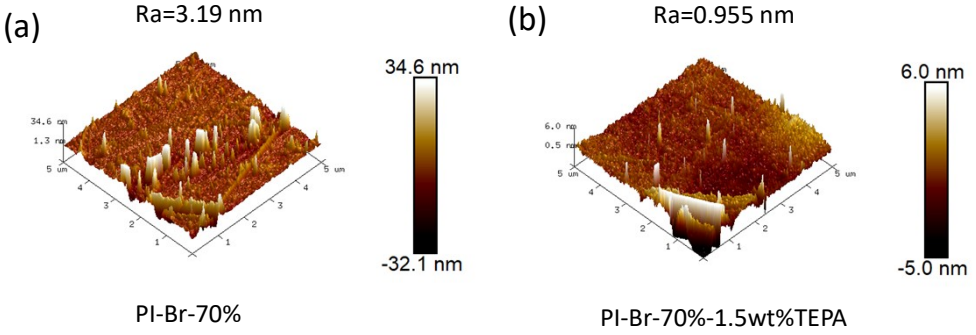

Fig. S1. 3D AFM topographical images of the membrane surfaces. (a) The pristine PI-Br-70% precursor membrane and (b) the modified PI-Br-70%-1.5wt%TEPA membrane. Note the significant difference in the vertical Z-axis scales, demonstrating the topological planarization after surface functionalization.

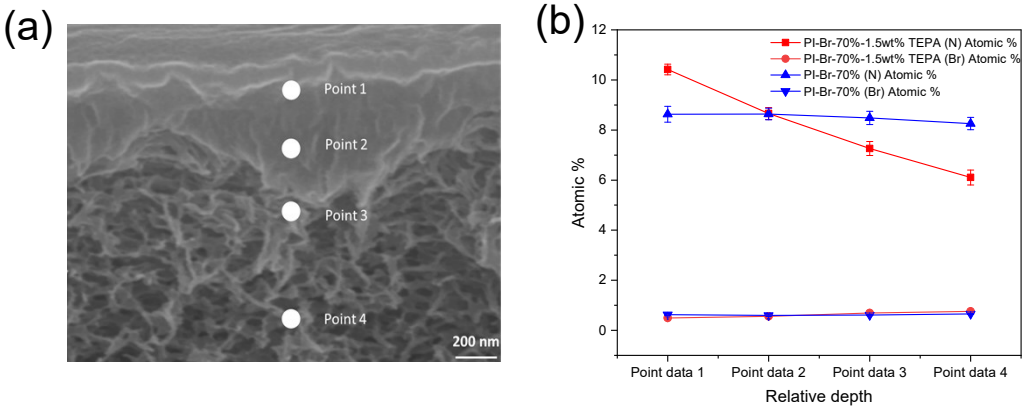

Fig. S2. Cross-sectional EDS depth profiling of the the membranes: (a) SEM image indicating the analysis locations from the dense layer to the porous support and (b) the variation of N and Br atomic concentrations.

Text S1. Evaluation of cross-linking density via gel fraction and swelling degree.

To quantitatively confirm the formation and density of the covalent cross-linking network induced by polyamine substitution, gel content and solvent swelling tests were conducted. Considering the surface-localized nature of the hollow fiber modification, fully bulk-cross-linked flat-sheet PI-Br-70% membranes were prepared as control models by prolonging the amination reaction time to ensure complete penetration and cross-linking.

The dried, pre-weighed membranes (Wd) were immersed in N,N-dimethylacetamide (DMAc) at room temperature for 24 h. Subsequently, the swollen membranes were carefully removed, wiped with filter paper to remove excess surface solvent, and weighed immediately (Ws). Finally, the samples were thoroughly dried in a vacuum oven at 80 °C to a constant weight and weighed again (Wg).

The swelling degree (SD) and gel fraction (GF) were calculated using the following equations:

$$SD(\%)=[(Ws-Wg)/Wg]\times 100\%$$

$$GF(\%)=(Wg/Wd)\times 100\%$$

During the test, the pristine, un-cross-linked PI-Br-70% flat-sheet membrane completely dissolved in DMAc within a few minutes, demonstrating a lack of network structure. Conversely, the TEPA-cross-linked flat-sheet membrane maintained its structural integrity after 24 h of immersion. The measured gel fraction reached 86.5%, while the swelling degree was restricted to 15.3%. These results provide direct macroscopic evidence of a dense and robust interchain covalent network imparted by the multifunctional TEPA carriers.

Table S2 Comparison of CO_2/N_2 separation performance.

Membrane	CO_2 permeance(GPU)	Test conditions	CO_2/N_2Selectivity	References
PDMS/PEI TFC-HFs	51	25℃;0.1MPa; Pure gas; No humidification	21	[14]
Nanoconfined Ionic Liquid membrane	1654	70℃;1.01bar 4.2% CO_2 + Saturated water vapor	1132	[35]
TpPa-SO_3H-DETA/COFs MMMs	2347	90℃；0.1MPa 10 vol% CO_2+ Saturated water vapor	191	[51]
PSf/GO/Pebax®1657 TFC HFMs	28	25℃;0.1MPa; Pure gas; No humidification	43	[52]
CTA/CDA HFMs	45	25℃;0.1MPa; Pure gas; No humidification	30	[53]
Poly(4-methyl-1-pentene)(PMP)	68	25℃;0.1MPa; Pure gas; No humidification	13.5	[54]
SSMMP-NH_2/PDMS	575	25℃;4 bar; Pure gas; No humidification	33	[55]
ZIF-8/PEI-600	3249	25℃;1 bar; Pure gas; No humidification	34	[56]
CAB-MWCNTs	377	25℃;3 bar; Pure gas; No humidificatio	13	[57]

Continued Table S2 Comparison of CO_2/N_2 separation performance.

Membrane	CO_2 permeance(GPU)	Test conditions	CO_2/N_2Selectivity	References
PAN HFMs	266.2	25℃;4 bar; Pure gas; No humidificatio	4.3	[58]
ArgK-PEI/PVC HFMs	488	35℃;0.2 bar; Pure gas; humidificatio	41	[59]
MOF-COF HFMs	352	25℃;0.1 bar; Pure gas; humidificatio	75	[60]
PES-PDMS/TFC HFMs	2150	25℃;0.1MPa; Pure gas; No humidification	20	[61]
PDMS-PEG HFMs	2667	25℃;3 bar; Pure gas; humidificatio	21	[62]
PI-Br-70%-TEPA HFMs	1362	25℃;0.2MPa; Pure gas; humidification	65	This work

Abbreviations

The following abbreviations are used in this manuscript:

HFMs: Hollow fiber membranes

TFC: Thin-filmcomposite

PDMS: Polydimethylsiloxane

PEI: Polyethylenimine,Polyetherimide

PES: Polyethersulfone

PSF: Polyphenylsulfone

CTA: Cellulosetriacetate

GO: Grapheneoxide

References

14. L. Shi, Y. Ma, Z. Chen, Y. Wang, Z. Qin, M. Deng, Y. Wang, L. Yang, L. Yao, J. Zheng, W. Jiang and Z. Dai,*Sep. Purif. Technol.*, 2025, 379, 134886.

35. F. Wang, D. K. Behera, B. Sengupta, D. Li and M. Yu, *Sci. Adv.*, 2026, 12, eaea1329.

51. L. Wang, Y. Zhou, S. Zha, S. Zhang and J. Jin, *ACS Sustain. Chem. Eng*., 2024, 12, 18475-18484.

52. R. A. Roslan, W. J. Lau, G. S. Lai, A. K. Zulhairun, Y. F. Yeong, A. F. Ismail and T. Matsuura, *Membranes*, 2020, 10, 335.

53. A. Raza, M. Askari, C. Z. Liang, N. Peng, S. Farrukh, A. Hussain and T.-S. Chung, *J. Membr. Sci*., 2021, 625, 119124.

54. A. V. Dukhov, M. Pelzer, S. Y. Markova, D. A. Syrtsova, M. G. Shalygin, T. Gries and V. V. Teplyakov, *Fibers*, 2022, 10, 1.

55. H. Z. Ferrari, C. Le Roux, F. L. Bernard, G. Dias, L. M. Dos Santos, P. Micoud, S. Mazières, F. Martin and S. M. O. Einloft, *ACS Omega*, 2026, 11, 6477 - 6499.

56. P. Li, D. Ao, Z. Gu, Z. Qiao and C. Zhong, J. Membr. Sci., 2026, 743, 125183.

57. Z. A. Jawad, R. J. Lee, V. Khosravi, A. L. Ahmad, H. B. Chua and S. P. Yeap, *Results Eng.*, 2025, 25, 104344.

58. A. Jana and A. Modi, J. Environ. *Chem. Eng*., 2026, 14, 122332.

59. L. Shi, Y. Ma, Z. Chen, Y. Wang, Z. Qin, M. Deng, Y. Wang, L. Yang, L. Yao, J. Zheng, W. Jiang and Z. Dai, *Sep. Purif. Technol.*, 2025, 379, 134886.

60. O. Choi, K. A. Veetil, C. H. Park, H. Kim and T.-H. Kim, *Chem. Eng. J*., 2024, 497, 154746.

61. B. Zhao, J. W. Wong, C. Z. Liang, J. Wu, T.-S. Chung and S. Zhang, *Sep. Purif. Technol*., 2023, 323, 124439.

62. F. Hillman, K. Wang, C. Z. Liang, D. H. L. Seng and S. Zhang, *Adv. Mater*., 2023, 35, 2305463.